CHALMERS

CFD Simulation of Flue Gas Flow in Traditional Indonesian Pottery Furnace

Numerical Study of Heat and Mass Transfer Phenomena, Radiation and Evaporation

Master of Science Thesis

KRISTINA NILENIUS

Department of Chemical and Biological Engineering
Division of Chemical Reaction Engineering
CHALMERS UNIVERSITY OF TECHNOLOGY

Göteborg, Sweden, 2011

CFD Simulation of Flue Gas Flow in Traditional Indonesian Pottery Furnace

Numerical Study of Heat and Mass Transfer Phenomena, Radiation and Evaporation

KRISTINA NILENIUS

Examiner:
Professor Bengt Andersson, Chemical Reaction Engineering, Chalmers University of Technology

Supervisor:
Professor Muslikhin Hidayat, Gadjah Mada University
Professor Rahman Sudiyo, Gadjah Mada University

Master of Science Thesis

Department of Chemical and biological engineering
Division of Chemical Reaction Engineering
CHALMERS UNIVERSITY OF TECHNOLOGY
Göteborg, Sweden 2011

CFD Simulation of Flue Gas Flow in Traditional Indonesian Pottery Furnace
Master thesis
KRISTINA NILENIUS
Department of Chemical and Biological engineering
Division of Chemical Reaction Engineering
Chalmers University of technology

Abstract

The production of pottery is an important industry on Java, Indonesia. The current process is very traditional and has been the same for many generations, which unfortunately means that the process of producing pottery can be regarded as obsolete and needs improvement. The temperature in the furnaces is too low for the vitrification process to begin and this is partially due to the fuel used. The current fuel used is firewood that has a low calorific value and a transition to briquettes made from rice husk or coconut shell need to happen since these fuels have a higher calorific value. The purpose of this project is to design a new and improved pottery furnace and to perform CFD simulations in order to increase the understanding of how the flue gas flow behaves inside the furnace. Other purposes are to develop a method to simulate evaporation of bounded water at the surface of the pottery and to predict radiation between the potteries. Evaporation is simulated with one reaction for adsorption and one reaction for desorption in equilibrium, the time when equilibrium is obtained was calculated using Matlab. The inlet temperature was set to 1073K in the simulations.

The results from the CFD simulation show a slightly uneven temperature distribution inside the furnace due to inertia movement of the flue gas flow. 22% of the initially bounded water evaporated during the 1100sec simulation and the reaction rates close to equilibrium reached 8.415 mole/m^2s for the absorption and 8.431 mole/m^2s for the desorption. Radiation has a great impact on the evaporation of water and should not be neglected even at lower temperatures. Further work with the obtained model could include a baffle to break the inertia movement and more detailed approximation of the pottery.

The project also has a great cultural aspect since four month was spent in Indonesia in order to understand the process of producing pottery. The traditional process of producing pottery has large limitations in available construction material and fuel but some traditional furnaces had a slightly modern design. Some obstacles in planning the construction of the furnace were mapped and smooth collaboration between academics and pottery makers was found to be a necessity.

Table of Contents

Acknowledgement

This project was made possible by the Internationella programkontoret and the exchange program Linneaus-Palme and I am very grateful to be given the opportunity to do this Master thesis through their scholarship. I am also thankful for the additional scholarship I received from Chalmers Vänner and ÅForsk.

I would like to thank Professor Bengt Andersson and Professor's assistant Ronnie Andersson for their encouragement and great sources of ideas. I also want to thank Professor Claes Niklasson for helping me with the travel arrangements.

Four month of this project was spent in Indonesia, mainly in Yogyakarta and I would like to thank my supervisors Professor Muslikhin Hidayat and Professor Rahman Sudiyo at Gadjah Mada University, Yogyakarta, for their support. I would also like to thank Mr. Dedi Eko for his help with practical issues in Yogyakarta.

I would also like to thank Adrian for all his support and feedback throughout this project, you always put a positive spin on everything.

Finally, I want to thank my dear friends at Gadjah Mada University that welcomed me into their lives with open arms. Thank you Andrettiane (Dedy) Putranti, Masduki Hamid, Tya Theya, Raudati Hilda, Novi Laura, Candra Aji, Wyndha Hendra and Anton Wijaya!

1 Introduction

1.1 Background

Pottery is an important product produced in Indonesia but the producing techniques are unfortunately obsolete and the country's economy could improve significantly if some modernization could be made. One problem with the current production technique is the temperature in the furnaces that is not high enough, resulting in a product more similar to dried clay than ceramic. A higher temperature would give harder and denser pottery that could be made thinner, which would decrease the consumption of raw material.

Another challenge is Indonesia's decrease of firewood, which is the current fuel in traditional pottery furnaces. New techniques to make coal briquettes from rice husk or coconut shells have been developed and a transit from firewood to rice husk or coconut shell briquettes should be made. The briquettes contain a higher calorific value compared to wood, which is beneficial to achieve a higher temperature in the furnace.

The Ministry of Science in Indonesia has acknowledged this issue and granted money to Gadjah Mada University (UGM) in Yogyakarta to develop and construct a furnace with improved properties. Chalmers University of Technology (CTH) in collaboration with UGM will seek possible ways to improve the traditional pottery production in order to develop the process as well as environmental benefits.

1.2 Traditional pottery

There are two villages close to Yogyakarta with pottery production as the main source of income. One is Kasongan located just south of the city centre and the other one is Pundong which is located further south of Yogyakarta, close to the sea. A large variety of pottery is produced in the two villages; some urns have a height of almost 2m and some has a height of 2dm. Some products have practical uses and some pottery is purely decoration. In Pundong it is common to produce very small pottery in batch sizes of thousands which are given away as gifts to wedding guests.

Some products are for domestic sell and some products are exported, especially to Australia but also to European countries and other Asian countries.

1.3 Traditional furnace design

The traditional pottery furnace has a square shape with an open roof. The roof is covered with a layer of straw that in turn is covered by a layer of tile. It is fired as an updraft furnace, the fireplace is below the load and the hot flue gases passes through the furnace from under and exits at the top. This is the most common type of traditional pottery furnaces used in Kasongan and Pundong but a slightly more modern version does however exist in Pundong where the furnace has a roof and a chimney. This type of furnace is a downdraft furnace where the hot flue gases from the fireplace passes through a firewall, enters the

furnace from above and exits at the bottom. An example on a traditional updraft furnace can be viewed in Figure 1 and the more modern, downdraft, version can be viewed in Figure 2.

Figure 1 Traditional updraft pottery furnace

Figure 2 A slightly more modern version of a traditional pottery furnace that has downdraft.

The benefits of a downdraft furnace are of importance. The vertical temperature distribution will be more even in the downdraft furnace since the flue gases exits from the bottom through a chimney that due to natural convection will give a natural circulation in the furnace. In an updraft furnace the hot flue gases causes hot plumes on the floor and cold areas between them which gives an uneven temperature distribution close to the floor.

1.4 Production of traditional pottery

The production of traditional pottery starts with mixing clay with sand and water. It is very important to get a homogenous mixture otherwise the risk of cracks and uneven quality will increase. The mixture is formed into its desired shape and size and is set to dry before fired. The dry but not fired body is called a green body. The green body is dried outside for 3-4 days depending on whether it is dry season or wet season. It is important that the bodies are not dried directly under the sun but in the shadow.

The green bodies are densely packed in the furnace, smaller bodies fills the voids between the larger ones. The furnaces are never fired half empty and the pottery maker prefers to wait until the batch size of green bodies is large enough to fill the entire furnace. An example of the dense packing is showed in Figure 3.

Figure 3 A densely packed furnace covered with a layer of tile but no straw. Everything is packed randomly and small items are placed between bigger ones.

The burning starts early in the morning and the temperature are initially increased slowly, if the temperature increases to fast then the pottery will crack. Traditional furnaces have two channel shaped inlets that are fired at equal rate. During the preheating period, the fire is held outside the inlet and is slowly pushed into the inlets. The feeding rate will increase throughout the burning and eventually the pottery will start to "glow", at this point, the feeding will stop and the fire will burn out. The firing is stopped after approximately 8 hours and it takes several hours for the pottery to cool down. The pottery needs to be completely cool before the furnace is unloaded.

The quality of the finished product is controlled and occasional cracked pottery is sorted out before the pottery is painted or glazed.

1.5 Aim of project

The process of producing pottery in Indonesia needs to be improved in many ways. The Ministry of Science has granted money to the project, which needs to be spent carefully and wisely. It is possible to build a new and more modern furnace and this furnace needs to be designed and analyzed. This hypothetical furnace will be developed using CFD and used to answer general questions regarding the

burning process and to increase the understanding of how the furnace behaves. It is also of interest to find a way to simulate evaporation of bounded water and radiation.

The cultural aspects of this project are considerable since a large part is conducted in Indonesia. It is important to find a beneficial collaboration between the pottery maker and academics from UGM and CTH. The issue of finding a traditional pottery maker willing to try new ideas should not be underestimated.

It is also of importance to investigate the necessary change of fuel further and to encourage the pottery makers actively to make the transition.

1.6 Limitations

When designing the new furnace considerations regarding building techniques had to be taken as well as available building materials. It was not possible to design the optimal furnace from strictly a technical point of view because the most modern materials are too expensive. Another important approach is that the most inefficient furnace is an unused furnace, meaning that if the new furnace is too different and foreign to the pottery makers then they will not use it. The development of Indonesia's pottery production needs to be taken step by step.

1.7 Objective

The objective for this project is to design a new furnace and to perform CFD simulations to predict the flue gas flow.

- Understand the behavior of the burning process
    - How is the flue gas flow inside the furnace behaving?
    - Is the downdraft within the furnace enough to get a satisfying temperature profile?
    - How could the model be further developed?
- Develop a method to simulate the burning process
    - How could the radiation within the furnace be simulated?
    - How could the evaporation of the bounded water be simulated?
    - Discuss how pottery can be approximated in the model
    - Investigate the temperature profile in order to make sure that the construction material will endure the stresses and to obtain an even quality of the pottery.
    - Simulate the radiation from the walls as well as the pottery
    - Simulate the evaporation of water from the surface of the pottery
- Investigate the possibilities to build the designed furnace and map the obstacles.
- Discuss the options to make the transition from firewood to briquettes made from rice husk or coconut shell.

2 Theory

This chapter is divided into three theory parts to increase the knowledge about the performed project. The first part is CFD theory, the second part is heat transfer theory and the third part is pottery theory.

2.1 CFD

In simulation of turbulent flows, computational fluid dynamics (CFD) is a very powerful tool with many applications. It gives detailed local information of the simulated system, which improves a qualitative understanding of the process. CFD solves Navier-Stokes (N.S.) equations numerically in an iterative way, N.S. equations describes the momentum transport of flows. Laminar flows can often be described very accurate with CFD simulation since it is dominated by viscous forces. N.S. also describes turbulent flows but the properties are too complicated to be solved for with CFD in any real engineering applications. The turbulent flow has a very large range of time scales, which makes direct solving of N.S. (DNS) only applicable for small systems and the turbulent flow has to be modeled in some way for larger systems. For these larger and more complex systems one method used frequently is Reynolds Average Navier Stokes (RANS) where the turbulent fluctuations are averaged resulting in simulations with sufficient result on scales larger than the grid. Limitations with RANS include scales smaller than the grid that remains unsolved for, i.e. mixing of chemicals or drops in turbulent flows. (1)

2.1.1 Governing transport equations

Some assumptions must be made in solving fluid flows. The flow is assumed incompressible which is defined as no variation in density along the streamline and this assumption reduces the equation of continuity to equation (2.1.1). The flow is also assumed to be considered as a Newtonian fluid. For a Newtonian fluid, the viscous stress is a linear function of the rate of strain and this is true for most common fluids such as gas or water where the viscous stress can be written as equation (2.1.2). Based on these assumptions the equation of motion is written as equation (2.1.3). Note that *i* and *j* denote the tree dimensions. In equation (2.1.3) the first term describes accumulation, the second term describes convection, the third term describe rate of change of pressure due to motion, the fourth term describes diffusion and the last term is the source term.

$$\frac{\partial U_j}{\partial x_j} = 0 \tag{2.1.1}$$

$$\tau_{ij} = \tau_{ji} = -\mu\left(\frac{\partial U_i}{\partial x_j} + \frac{\partial U_j}{\partial x_i}\right) \tag{2.1.2}$$

$$\frac{\partial U_i}{\partial t} + U_j\frac{\partial U_i}{\partial x_j} = -\frac{1}{\rho}\frac{\partial P}{\partial x_i} + \mu\frac{\partial}{\partial x_j}\left(\frac{\partial U_i}{\partial x_j} + \frac{\partial U_j}{\partial x_i}\right) + G_i \tag{2.1.3}$$

These equations are solved numerically by CFD software by dividing the computational domain into cells and thus reformulate them from partial differential equations to algebraic equations. This reformation also leads to numerical errors and the magnitude of these errors depends of the cell size. A smaller cell size will decrease the error but increase the computational time, which is costly. When working with CFD a compromise between accuracy and expense must always be made. (1)

2.1.2 Turbulence modeling

A turbulent flow greatly enhances the heat and mass transfer rates compared to laminar flow, which is why the turbulent flow is suitable in industrial applications. Modeling of the turbulent flow is thus an important element in CFD aided chemical engineering. Turbulent flow has some characteristic features, it is irregular and consist over a wide range of turbulent eddies and it is diffusive due to the chaotic motion. The turbulent flow is highly instable and random at large Reynolds numbers even though the N.S. equations are deterministic, it is also intrinsically tree-dimensional since vortex stretching and vortex tilting cannot occur in two dimensions. Another characteristic is dissipation of turbulent energy commonly referred to as the energy cascade where the energy enters the turbulence at the larger scale and by inviscid processes is transferred into smaller and smaller turbulent scales until it dissipates by viscosity. (1)

2.1.3 Reynolds decomposition

To reduce and simplify the information about the turbulent flow statistical methods are used, Reynolds was the first to introduce this concept in Reynolds decomposition. In Reynolds decomposition, the velocity is divided into its mean and fluctuating part as in equation (2.1.4) where the mean velocity is defined as in equation (2.1.5).

$$U_i = \langle U_i \rangle + u_i \tag{2.1.4}$$

$$\langle U_i \rangle = \frac{1}{2T}\int_{-T}^{T} U_i dt \tag{2.1.5}$$

With Reynolds decomposition, the flow can be considered as randomly varying components affecting a mean flow. The intensity of the velocity fluctuation can be measured by the turbulent kinetic energy per unit mass according to equation (2.1.6) where 1, 2 and 3 denotes the three dimensions. The kinetic energy in a specific point is described by equation (2.1.7) which can be decomposed according to equation (2.1.8).

$$k = \frac{1}{2}(\langle u_1^2 \rangle + \langle u_2^2 \rangle + \langle u_3^2 \rangle) \tag{2.1.6}$$

$$E = \frac{1}{2} U_i U_i \tag{2.1.7}$$

$$\langle E \rangle = \frac{1}{2}\langle (\langle U_i \rangle + u_i)(\langle U_i \rangle + u_i) \rangle = \frac{1}{2}(\langle U_i \rangle \langle U_i \rangle + \langle u_i \rangle \langle u_i \rangle) = \bar{E} + k \tag{2.1.8}$$

The pressure also has to be decomposed in a similar way for incompressible flows but there is no need to decompose other quantities besides these to solve the N.S. equations. For compressible flows, the density must also be decomposed. (1)

2.1.4 Reynolds Averaged Navier Stokes equation

Several turbulence models are based on Reynolds decomposition and these are denoted Reynolds Averaged Navies Stokes equations (RANS equations). Using the Reynolds decomposition N.S. equations can be written as in equation (2.1.9) which is the general form for RANS-equations. Note the term $\rho\langle u_i u_j \rangle$ that is the Reynolds stresses which introduces a coupling between the mean and fluctuating

parts of the velocity field. The modeling of the Reynolds stress term is the sole purpose of RANS turbulence modeling. RANS turbulence models closes the N.S. equations with an adequate balance between accuracy and computational time and this project is based on two of these models, the k-ε model and the k-ω model. (1)

$$\frac{\partial\langle U_i\rangle}{\partial t}+\langle U_i\rangle\frac{\partial\langle U_i\rangle}{\partial x_j}=-\frac{1}{\rho}\frac{\partial}{\partial x_j}\left\{\langle P\rangle\delta_{ij}+\left(\frac{\partial\langle U_i\rangle}{\partial x_j}+\frac{\partial\langle U_j\rangle}{\partial x_i}\right)-\rho\langle u_iu_j\rangle\right\} \quad (2.1.9)$$

2.1.5 The Boussinesq approximation

In modeling the Reynolds stress term that closes N.S. equations, the Boussinesq approximation is used in several RANS turbulence models. The Boussinesq approximation assumes that the components of the Reynolds stress term are proportional to the mean velocity gradients. This assumption implies that the Reynolds stresses can be modeled analogous to molecular viscosity with a turbulent viscosity also denoted eddy viscosity. The Boussinesq approximation is written as in equation (2.1.10). The analogy to molecular viscosity leads to some limitations for the Boussinesq approximation when predicting simple flows as for example channel flows but it is still considered to be very cost effective which is a great benefit. (1)

$$\frac{\tau_{ij}}{\rho}=-\langle u_iu_j\rangle=\nu_T\left(\frac{\partial\langle U_i\rangle}{\partial x_j}+\frac{\partial\langle U_j\rangle}{\partial x_i}\right)-\frac{2}{3}k\delta_{ij} \quad (2.1.10)$$

2.1.6 Two equation models

For most CFD simulation in real engineering applications, two equation models are used to determine the velocity and length scales that describe the local turbulence and thereby close the RANS- equations with the eddy viscosity concept. Two equation models solves the *k*-equation for the velocity scale and the *l*-equation for the length scale, quite often an alternative property than the length scale is solved for in the second equation providing it is possible to explicitly determine the length scale from this property. The two equation models have some limitations but they are quite favorable due to their robustness and inexpensiveness. (1)

2.1.7 The k-ε model

The k-ε model is a robust and easily interpreted model and it is widely used in many practical engineering flow simulations. It does however impose some limitations in predicting flows with streamline curvature, swirling flows and axisymmetrical jets. The *k*-ε model was derived for flows with high Reynolds numbers and is not the best choice for regions with low Reynolds number. The k-equation is written in equation (2.1.11) and to close this equation the energy dissipation rate, ε, has to be modeled with a second transport equation (2.1.12). (1)

$$\frac{\partial k}{\partial t}+\langle U_j\rangle\frac{\partial k}{\partial x_j}=\nu_T\left[\left(\frac{\partial\langle U_i\rangle}{\partial x_j}+\frac{\partial\langle U_j\rangle}{\partial x_i}\right)\frac{\partial\langle U_i\rangle}{\partial j}\right]-\varepsilon+\frac{\partial}{\partial x_j}\left[\left(\nu+\frac{\nu_T}{\sigma_k}\right)\right]\frac{\partial k}{\partial x_j} \quad (2.1.11)$$

$$\frac{\partial \varepsilon}{\partial t}+\langle U_j\rangle\frac{\partial \varepsilon}{\partial x_j}=C_{\varepsilon1}\nu_T\frac{\varepsilon}{k}\left[\left(\frac{\partial\langle U_i\rangle}{\partial x_j}+\frac{\partial\langle U_j\rangle}{\partial x_i}\right)\frac{\partial\langle U_i\rangle}{\partial j}\right]-C_{\varepsilon2}\frac{\varepsilon^2}{k}+\frac{\partial}{\partial x_j}\left[\left(\nu+\frac{\nu_T}{\sigma_\varepsilon}\right)\right]\frac{\partial \varepsilon}{\partial x_j} \quad (2.1.12)$$

2.1.8 The k-ω model

When modeling regions with low turbulence the k-ω model has very good performance, it is also reliable to predict the law of the wall and thereby eliminate the need for wall functions. It does however requires a fine mesh close to the grid with the first grid below y^+=5. The *k*-equation is written as is equation (2.1.13) and the ω-equation is written as in equation (2.1.14) where ω is the specific dissipation which is the inverse of the time scale denoted$\omega \propto \varepsilon/k$. The turbulent viscosity is calculated from equation (2.1.15). (1)

$$\frac{\partial k}{\partial t} + \langle U_j \rangle \frac{\partial k}{\partial x_j} = \nu_T \left[\left(\frac{\partial \langle U_i \rangle}{\partial x_j} + \frac{\partial \langle U_j \rangle}{\partial x_i} \right) \frac{\partial \langle U_i \rangle}{\partial j} \right] - \beta k\omega + \frac{\partial}{\partial x_j} \left[\left(\nu + \frac{\nu_T}{\sigma_k} \right) \right] \frac{\partial k}{\partial x_j} \quad (2.1.13)$$

$$\frac{\partial \omega}{\partial t} + \langle U_j \rangle \frac{\partial \omega}{\partial x_j} = \alpha \frac{\omega}{k} \nu_T \left[\left(\frac{\partial \langle U_i \rangle}{\partial x_j} + \frac{\partial \langle U_j \rangle}{\partial x_i} \right) \frac{\partial \langle U_i \rangle}{\partial j} \right] - \beta^* \omega^2 + \frac{\partial}{\partial x_j} \left[\left(\nu + \frac{\nu_T}{\sigma_\omega} \right) \right] \frac{\partial \omega}{\partial x_j} \quad (2.1.14)$$

$$\nu_T = \frac{k}{\omega} \quad (2.1.15)$$

2.1.9 SST model

The SST model uses the *k*-ω model in the bounded wall region and the *k*-ε model for the free stream thus combining the strength of both models without being computationally expensive. It requires fine mesh close to the wall but no wall functions. (1)

2.1.10 Mesh

Meshing is an important part in working with CFD since an inadequate mesh can for example cause longer computational time and numerical diffusion. Grids can be divided into structured and unstructured grids where the structured grids are build up by quadrilateral element while unstructured grids are build from different element, for example quadrilateral and triangular elements. The structured grids are resolved faster, require less memory and have better numerical properties. For complex geometries, it is not always possible to mesh only using structured mesh and solvers must be able to handle both.

The area near walls must be handled carefully and the angle between the wall and the grid line should be close to 90°. To avoid inaccurate solutions due to meshing adjacent cells should be of equal size and high skewness should be avoided since is leads to instabilities and lower accuracy. For long thin channels cells can be stretched along a coordinate axis, even though the aspect ratio are increased this will still be acceptable since the gradients are low in that direction. It is often good to use different grid spacing in different regions of the grid.

Complex regions often require a denser grid compared to free flow since areas with large gradients often contains larges errors. The grid can be refined or coarsened in an appropriate way to increase the accuracy of simulations performed. (1)

2.1.11 Reaction modeling

The evaporation of the bounded water is regarded as a surface reaction with one forward and one backward reaction in equilibrium. The reactions are laminar finite-rate where the turbulent fluctuations are ignored. The reaction rate is determined by the Arrhenius expression showed in equation (2.1.16).

$$k = AT^{\beta} e^{-E/RT} \qquad (2.1.16)$$

Where A=pre-exponential factor, ß=temperature exponent and E=activation energy (2)

2.1.12 User defined function - UDF

A user defined function is an external code often written in C++ that provides additional information to Fluent. In this project, a UDF is used to set the absorption coefficient in the firewall and in the porous bodies. The code can either be compiled or interpreted by Fluent and it was chosen to interpret the code in this project. The code can be viewed in appendix (8.1)

2.2 Heat transfer

The three basic mechanisms of heat transfer are conduction, convection and radiation. The fundamental equations will be described in this chapter and their rate of energy transfer will be evaluated. (2)

2.2.1 Conduction

There are two governing mechanisms in heat conduction. The first mechanism is molecular interaction where a temperature gradient is the driving force. The second mechanism is heat transfer by free electrons. This mechanism is significant in metals since the concentration of free electrons is high in metals but does not exist in nonmetallic solids. The equation describing heat conduction is referred to as Fourier's first law of heat conduction and is written as in equation (2.2.1) where *k* is the thermal conductivity and is independent of direction making this expression isotropic. (2)

$$\frac{q_x}{A} = -k\frac{dT}{dx} \qquad (2.2.1)$$

2.2.2 Convection

Heat convection involves heat transfer between a surface and an adjacent fluid and there exist two different types of convection; forced convection and free or natural convection. Forced convection implies an agent forcing the fluid past the solid such as a fan or a pump. Free or natural convection causes movement of the fluid by density difference resulting from the temperature variation in the fluid. The rate equation is referred to as the Newton rate equation and is written as in equation (2.2.2) where *h* is analogous to *k* in Fourier's law of heat conduction. (2)

$$\frac{q_x}{A} = h\Delta T \qquad (2.2.2)$$

2.2.3 Radiation

Heat transfer by radiation differs some compared to conduction and convection since no medium is required for its propagation. Stefan-Boltzmann law of thermal radiation describes the rate of energy emission from a perfect radiator referred to a black body and it is written as in equation (2.2.3) where σ is the Stefan-Boltzmann constant. Heat transfer by radiation is of great importance at high temperatures. (2)

$$\frac{q_x}{A} = \sigma T^4 \qquad (2.2.3)$$

2.3 Technology of Pottery

The technology behind pottery making is examined through investigations of the clay minerals, the importance of drying and reactions occurring during firing of the clay body.

2.3.1 The clay minerals

One important property of clay is its plasticity. Plasticity is characterized as a materials ability to deform easily when processed but does not deform once it has a desired shape. This property is derived from the clays mineral content. The most important clay mineral is kaolinite with the sum formula $Al_2(Si_2O_5)(OH)_4$ and it is derived from breakdown of the mineral feldspar or of similar minerals formed under high temperature.

The structure of kaolinite consist of a two layer silicate sheet structure in which the $(Si_2O_5)^{2-}$ has a tetrahedral geometry. These ions are made electrically neutral by the adjacent $Al_2(OH)_4^{2-}$ layer as shown in Figure 4. (3) However, the structure is rarely this perfect and disorder of the structure affects the ceramic properties. One group of kaolinitic clay is halloysite minerals that has the same sum formula as ideal kaolinite but differs structurally. Water molecules exist between the layers in halloysite minerals and this makes the mineral hydrated. The sum formula for halloysite minerals can expressed as $Al_2(OH_4)Si_2O_5 \cdot 2H_2O$. (4)

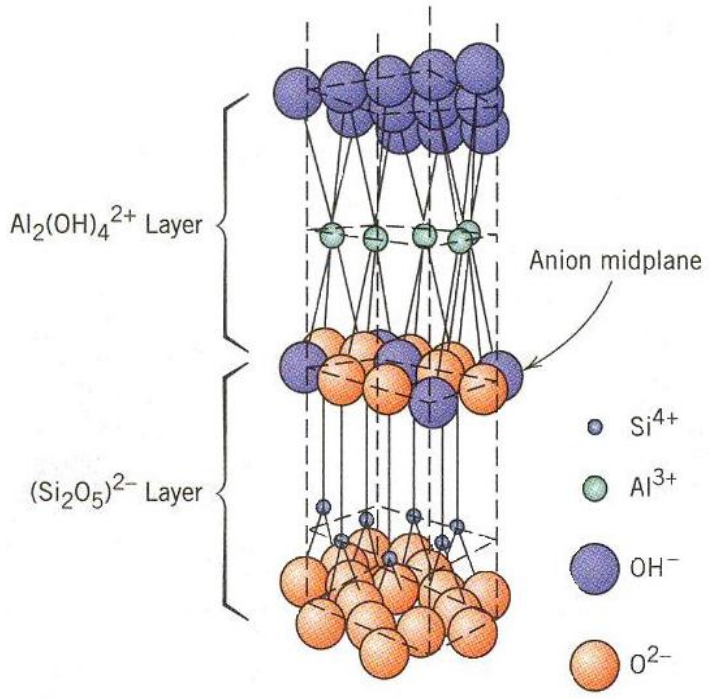

Figure 4 Structure of kaolinite clay (3)

2.3.2 Drying of clay

Drying of clay is an important step in turning a clay body into a ceramic ware. Water is often added during forming of the desired shape and as this liquid is removed during the drying process, density and strength is enhanced. A body that has been dried but not fired is called a green body. (4)

During drying, some shrinkage also occurs and this is due to removal of water initially surrounding the clay minerals. The rate of drying is also of importance since diffusion to the surface where evaporation occurs is rate controlling. If the rate of evaporation is higher than the diffusion rate, the surface will dry and shrink more rapidly than the interior, which increases the risk of cracks, distortion or warpage of the body. These stages of drying are shown in Figure 5. (3)

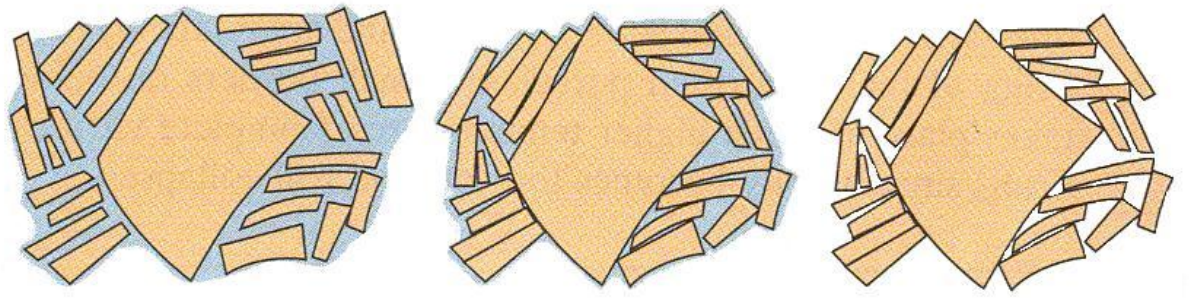

Figure 5 The stages of drying. The left one shows unbound moisture, the middle one bounded moisture and the right one shows the dry body. (3)

The thickness of the body also influences shrinkage because a thick body runs higher risk of non-uniform shrinkage that leads to deformation of the body. The initial water content of the body is obviously also of importance and should be kept as low as possible. (3)

2.3.3 Bounded and unbounded moisture content

The total moisture content in clay can be divided into bounded moisture and unbounded moisture. The unbounded moisture can be removed by saturated gas and the removal of this moisture is not the critical part of drying clay. The bounded moisture is the equilibrium moisture content at 100% humidity and at intermediate states of humidity the total moisture content can be divided into free moisture content and equilibrium moisture content. This relationship is illustrated graphically in Figure 6. The vapor pressure in equilibrium will be lower for bounded moisture compared to unbounded moisture. (5)

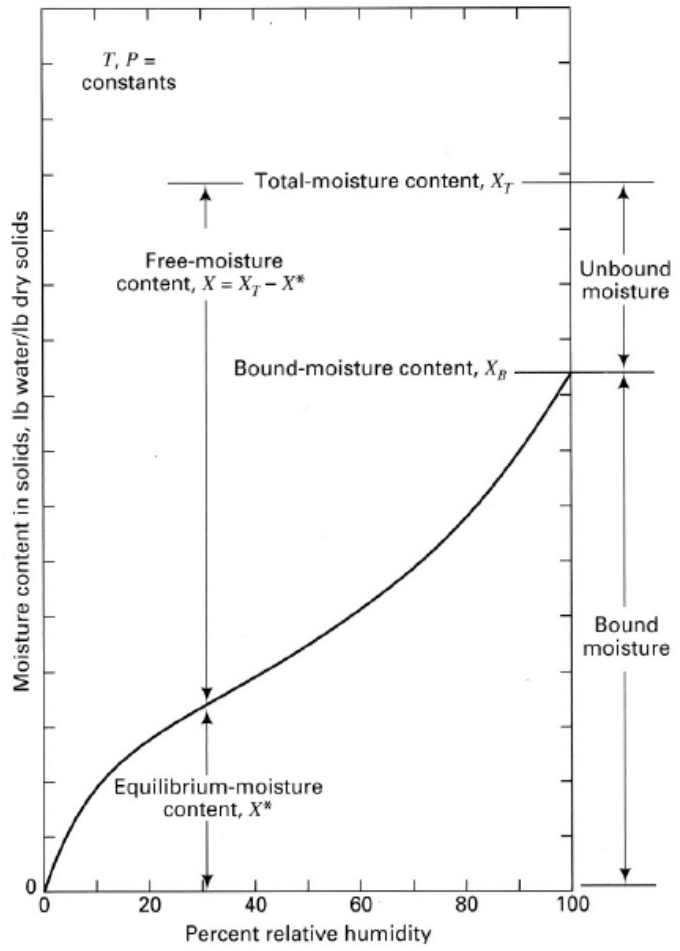

Figure 6 The relationship between free moisture content, equilibrium moisture content and bound moisture content. (5)

2.3.4 The action of heat on clay minerals

The clay minerals undergo several important steps while heated. At 420^{o}C the lattice of kaolinite will begin to break up due to evaporation of water, this process is endothermic and finishes at 550^{o}C leaving a non-crystalline material called meta-kaoline. At 900^{o}C an exothermic reaction occurs which is significant for the enhancement of the mechanical properties. This reaction is referred to as vitrification where gradual formation of a liquid glass takes place. The liquid glass flows into and fills some of the pore volume and the result after cooling is a dense, strong body. The degree of vitrification increases with increasing temperature, firing time and the body's composition. (3)

3 Method

3.1 CFD

The overall way of working while developing the model was done in an iterative and step-by-step way. Simulations was done and re-done as knowledge about the behavior increased and the simulations got more and more detailed and advanced. It is not necessary to present all steps in the development of the final model since they should only be considered as intermediate steps and not final models.

3.1.1 Overall development of the model

Some important crossroads are of interest during the development of the final model. The results from these simulations will be neglected to present since they were used only to develop the model further.

1. The geometry was altered by an increased inlet area.
2. The modeling of the firewall was refined.
3. Absorption of heat in the outer walls was added.
4. Simulation of radiation was added to the model.
5. The modeling of pottery was enhanced to become more detailed.
6. Evaporation was simulated thus changing the simulations from steady state to transient.

3.1.2 Development of the geometry

The geometry was created in the Design Modeler from the ANSYS Workbench platform. The outer dimensions of the furnace were decided through discussions and evaluations of existing furnaces. One conclusion was that the pottery batch size will remain unchanged and a larger internal surface area is not required, the height of existing furnaces were considered to be to low since some pottery cannot fit. The resulting dimensions are seen in Figure 7. Another important aspect was that most traditional furnaces are updraft furnaces. Since a downdraft furnace is much more preferable it was chosen to make the design as a downdraft furnace. The traditional furnaces also has two inlets but it was believed that one inlet was sufficient to give an even temperature profile. Since it is more difficult to control two fires, one inlet should be preferable if the simulations would give satisfying results.

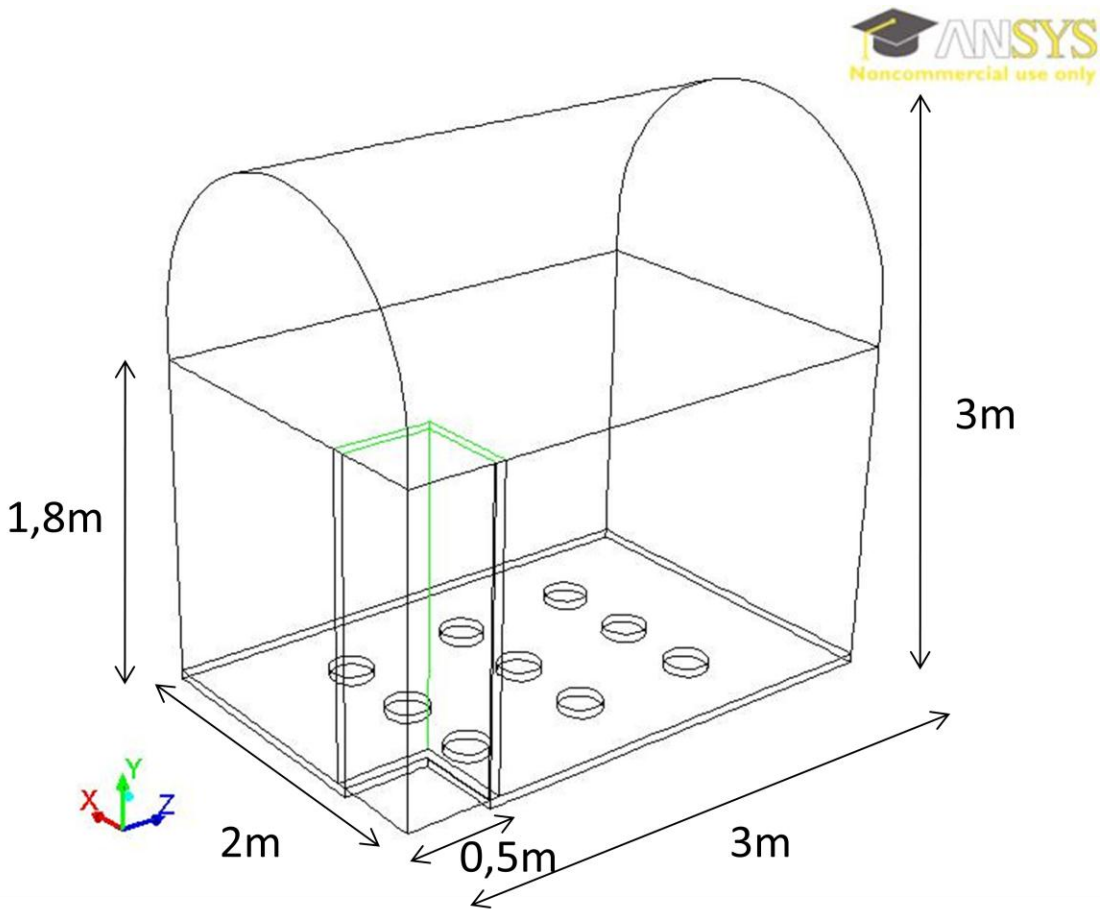

Figure 7 Outer dimension of the designed furnace.

The internal shape was developed using Fluent in a step-by-step procedure where the geometry was thoroughly investigated and then revised and redone until acceptable results were obtained.

In the first case, the inlet dimensions for the flue gases were set to 25x25cm and the height of the firewall was set to 1.8m. The total outlet area was set to 7% of the total floor surface area according to (6). It was later decided to increase the dimensions of the inlet to 50x50 cm but the other dimensions were kept unchanged. A third geometry was later developed which included a 7cm thick firewall. This geometry was considered as the final one.

The pottery was approximated with one large porous body with the height of 1.8m in the first approach. The reason for this crude approximation was to facilitate the simulations of the flue gas flow and see if the flow spread evenly throughout the space above the pottery giving an even temperature distribution.

A second approximation for the pottery was later made where the porous body was divided into several 40x40cm bodies with a distance between them. The reason was to investigate how radiation from one piece of pottery affected other facing pieces of pottery. The two pottery approximations are shown in Figure 8 and in Figure 9.

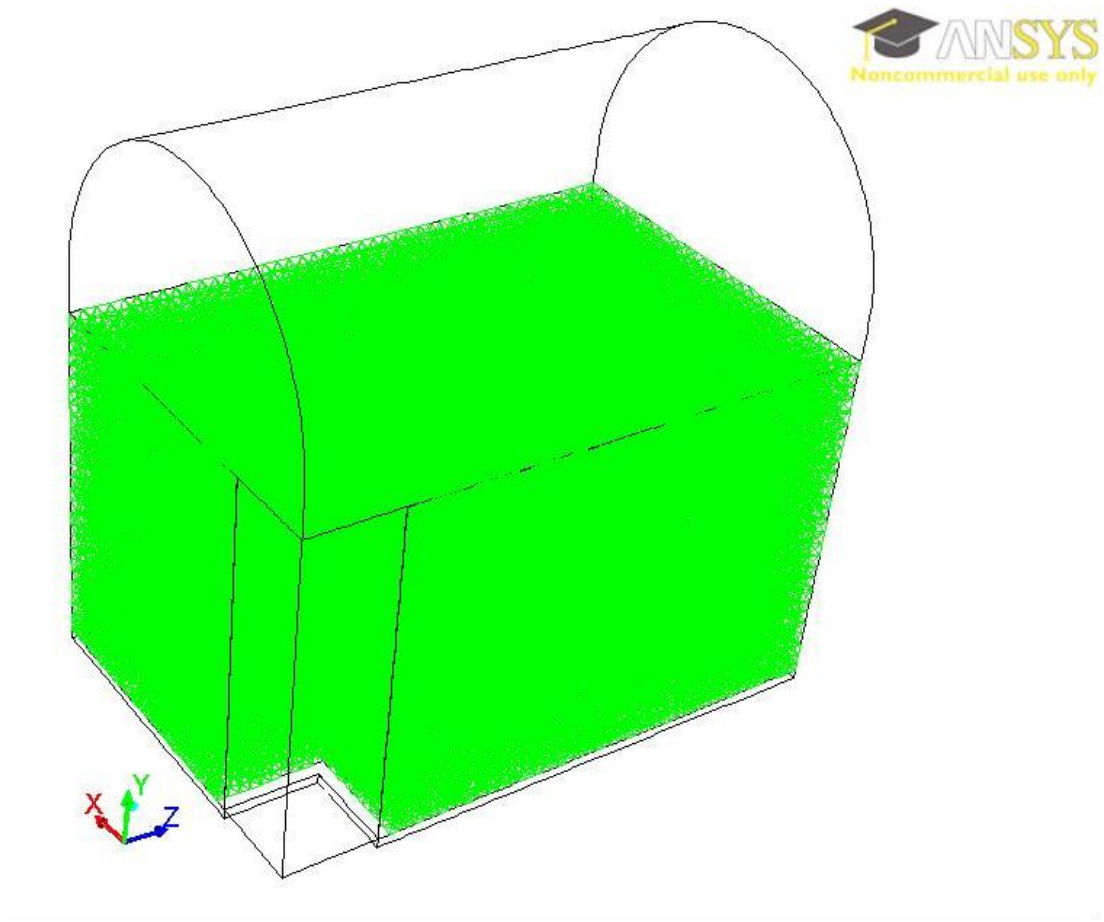

Figure 8 The first geometry where the pottery was approximated with one large porous body. The green space is the porous body.

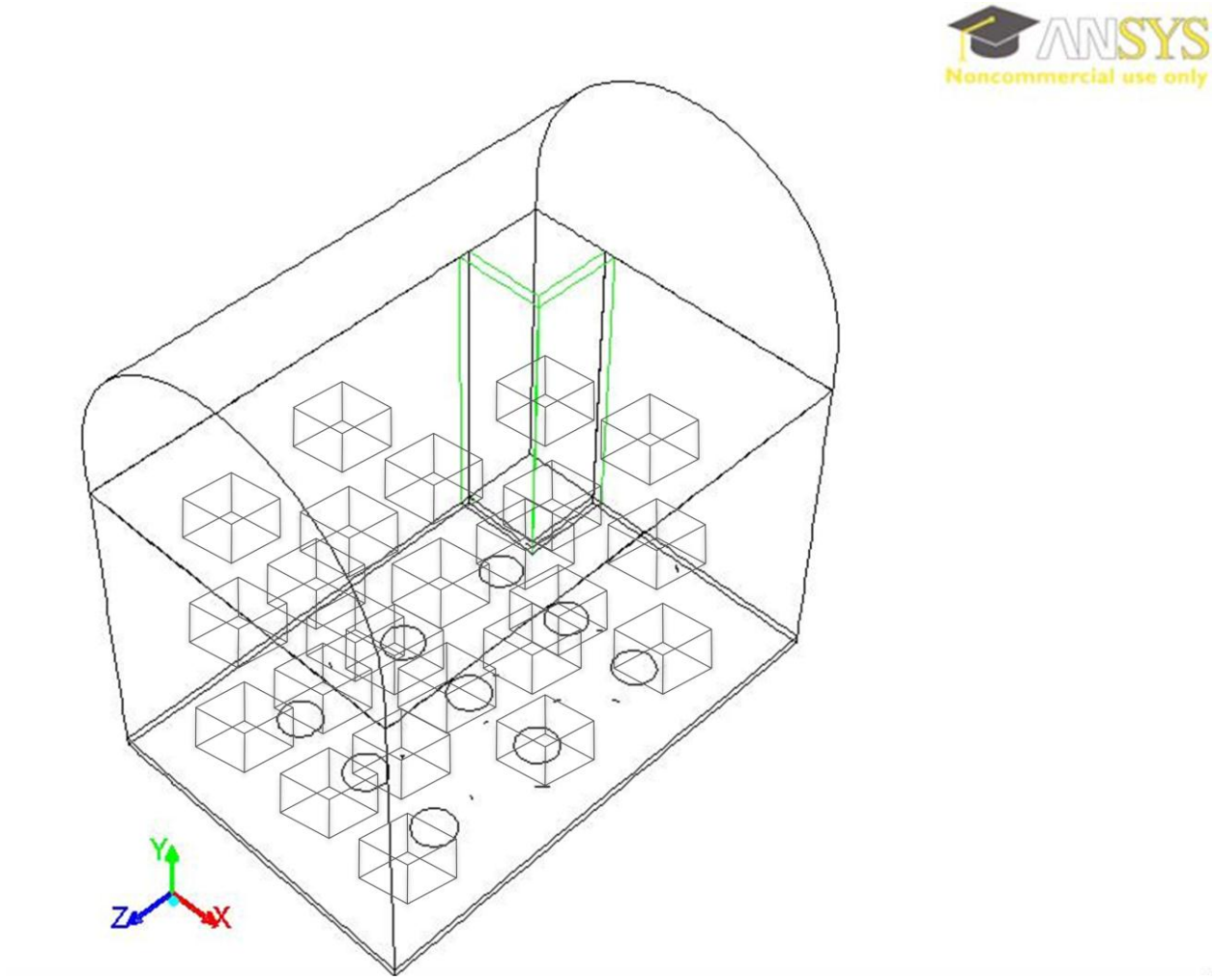

Figure 9 The second geometry where the pottery was approximated with several smaller bodies, 24 in total.

Two alternative geometries with baffles were also made. The first geometry had a small rectangular baffle and the second one had an arc shaped baffle. The simulations with these geometries can be considered as a sidetrack and is not further discussed since the geometry at a very early stage was used.

3.1.3 Mesh

The mesh was created in the meshing tool from the ANSYS Workbench platform. The inflation had a growth rate of 1,2 with a maximum layer of 5 cells. Curvature and proximity was chosen as size function. The mesh was later refined with y+ adaption and when evaporation was simulated the mesh was refined according to the gradient of turbulent viscosity. The number of cells in the final model was 631 175. The mesh in a plane through the porous bodies is displayed in Figure 10.

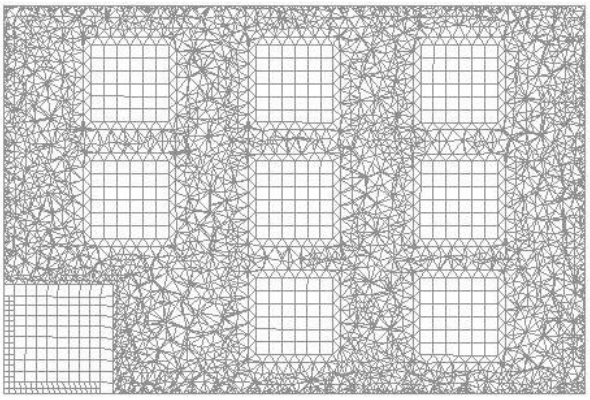

Figure 10 The mesh though the middle of the porous bodies.

The orthogonal quality is a measurement of the mesh quality with a number between 0 and 1 where 0 indicates low quality. (7) The critical areas around the porous bodies have an orthogonal quality number of 0.75-1 but it decreases to 0.5-0.6 in some areas close to the floor.

Cell skewness is another measurement of quality where the cell equivolume skew should not exceed 0.5 on a scale between 0 and 1. (7) Some occasional cells have a cell equivolume skewness of >0.5 but the overall values is <0.4 which indicates good cell quality.

3.1.4 Simulation

The turbulence flow model chosen was the SST model and all geometry alternatives were run with second order up-wind and with y+ adaption. The effects of radiation were encountered for with the Discrete Ordinate model. Radiation was encountered for in the geometry with one large porous body as well as in the geometry with several smaller bodies. Evaporation of water was first approximated as a heat sink in the porous body/bodies but this approximation is very crude and was later refined in a more advanced approximation.

3.1.5 Boundary conditions and settings

All outer walls as well as the roof were set as walls but the floor had to be set as porous body with zero velocity. The inlet is set as mass flow inlet and the outlet is set as pressure outlet. The firewall is set as porous body with zero velocity

In the first step where the pottery was approximated as a large porous body the porosity was set to 0.1, the heat sink to -4kW/m^3 and the resistance according to equation (3.1.1) where the length, *d*, was set to 5 cm in the y-direction and 3 cm in the x- and z-direction. It was assumed that the flue gases will flow easier around the pottery compared to through them and the resistance should therefore be higher in the x- and z direction compared to the y-direction.

$$\frac{\Delta P}{dx} = \frac{32\mu U}{d^2} \qquad (3.1.1)$$

In the second approximation with several smaller bodies, the resistance was increased to 3 cm in the y-direction and 2 cm in the x- and z-direction. The absorption coefficient was set to 1e5. When evaporation was simulated more in detail the velocity was set to zero in the porous bodies.

The inlet flow had a mass flow rate of 0.1417 kg air/s which corresponds to a linear velocity of 1.72 m/s. The inlet temperature had a temperature of 1073K. The mass inlet flow was calculated from the stoichiometric relationship of the coal content in the fed briquettes and a 100% excess air supply was assumed. The calculations of the mass flow can be found in appendix (8.3).

3.1.6 Simulation of radiation

The chosen model for simulation of radiation was the Discrete Ordinate (DO) model. All walls were set as participants in radiation as well as the firewall and porous bodies. The absorption coefficient was set to 1e5 in the firewall and in the porous bodies and it was set for both the material itself and for the gas inside the material. This high absorption coefficient was chosen because all radiation should be absorbed at the surface of the material. The flue gas was considered not to absorb or emit any radiation because of the low gas temperature.

3.1.7 Simulation of evaporation

The evaporation was approximated with one forward reaction for adsorption and one backward reaction for desorption in equilibrium. The expressions for the reaction rate of adsorption and desorption is written as in equation (3.1.2) and (3.1.3) where theta is the ratio of initial surface coverage of bounded water. Concentration and theta were solved for in Matlab using ode15s and the equations were written as in equation (3.1.4) and equation (3.1.5). The coefficients k_d and k_a were found with an iterative approach using Matlab, see Appendix (8.2).

$$r_{des} = k_d e^{\left(\frac{-\Delta H_{vap}}{RT}\theta\right)} \qquad (3.1.2)$$

$$r_{ads} = k_a cRT(1-\theta) \qquad (3.1.3)$$

$$\frac{dc}{dt} = \frac{-qc}{V} + (r_{des} - r_{ads})\frac{V_{bodies}}{V_{tank}} \qquad (3.1.4)$$

$$\frac{d\theta}{dt} = \frac{-(r_{des} - r_{ads})}{n_{h_2o}} \quad (3.1.5)$$

The evaporation simulations were run transient using a time step of 1 second for approximately 1100 seconds. To simulate the heat of evaporation in Fluent the activation energy was set to the value of the heat of evaporation for the two reactions. The activation energy for the adsorption reaction was set to zero since no energy is taken from the porous body to condensate already evaporated water. The activation energy for the reaction of desorption was set as 37,9kJ/mole which is approximately 1,5 times higher compared to the heat of evaporation for unbounded water at this temperature. It was estimated that it would require approximately 1,5 times more energy to evaporate bounded water compared to unbounded water.

The pre-exponential factor was set to 50 for the adsorption reaction and 600 for the desorption reaction. These numbers are not consistent with the conclusions from the Matlab simulation but it was necessary to make some alteration in order to obtain equilibrium between the reactions in Fluent.

4 Results

Results from the CFD simulations and the study period in Indonesia are presented.

4.1 CFD Results

All results and conclusions presented here are from the final version of the model. Keep in mind that CFD gives a model of reality, it is not a computer made picture of reality.

4.1.1 Temperature profiles

The temperature profiles show how inertia movement forces the flue gases along the arc shaped roof to the diagonal corner and thereby creating a colder area in the central part of the furnace, this can be viewed in Figure 11. It differs around 100°C between the center of the roof and areas closer to the walls. This gives a somewhat uneven temperature distribution inside the porous bodies and up to 80°C difference in temperature between the cores of the porous bodies.

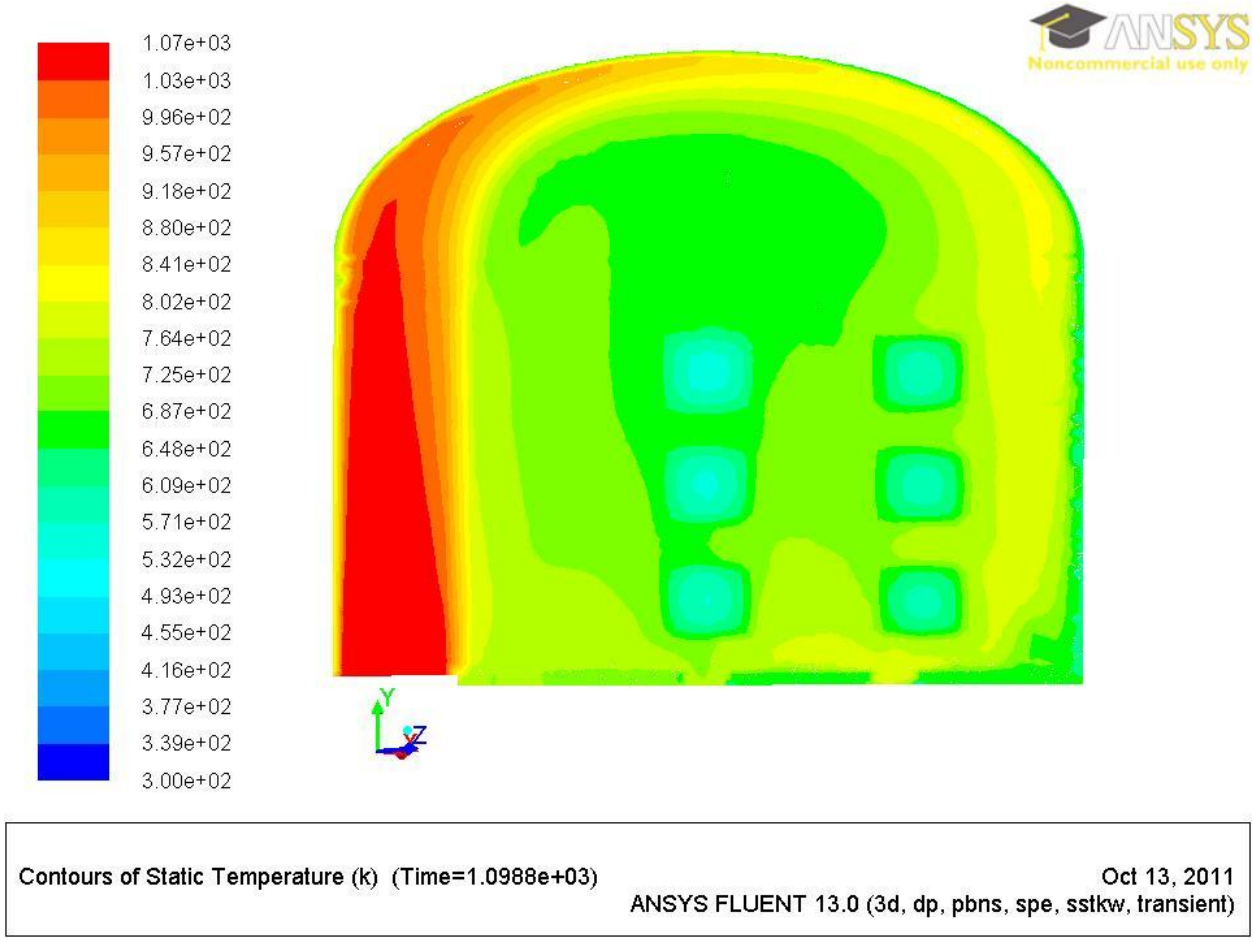

Figure 11 Temperature distributions inside the furnace. Diagonal view through the inlet to the opposite corner.

A more detailed view of the areas close to the walls shows that the walls are significantly cooled by emitting radiation and heat conduction through the walls. The cooled walls increase the downdraft in the furnace.

4.1.2 Radiation profile

By looking at the radiation profile, it is clear that radiation is significant even though the temperature in the furnace is quite low. The area that emits the most radiation is not surprisingly the inlet area where the temperature is the highest. Radiation between the porous bodies also exist and should not be neglected, the overall radiation profile is however not even between the porous bodies that Figure 12 indicates.

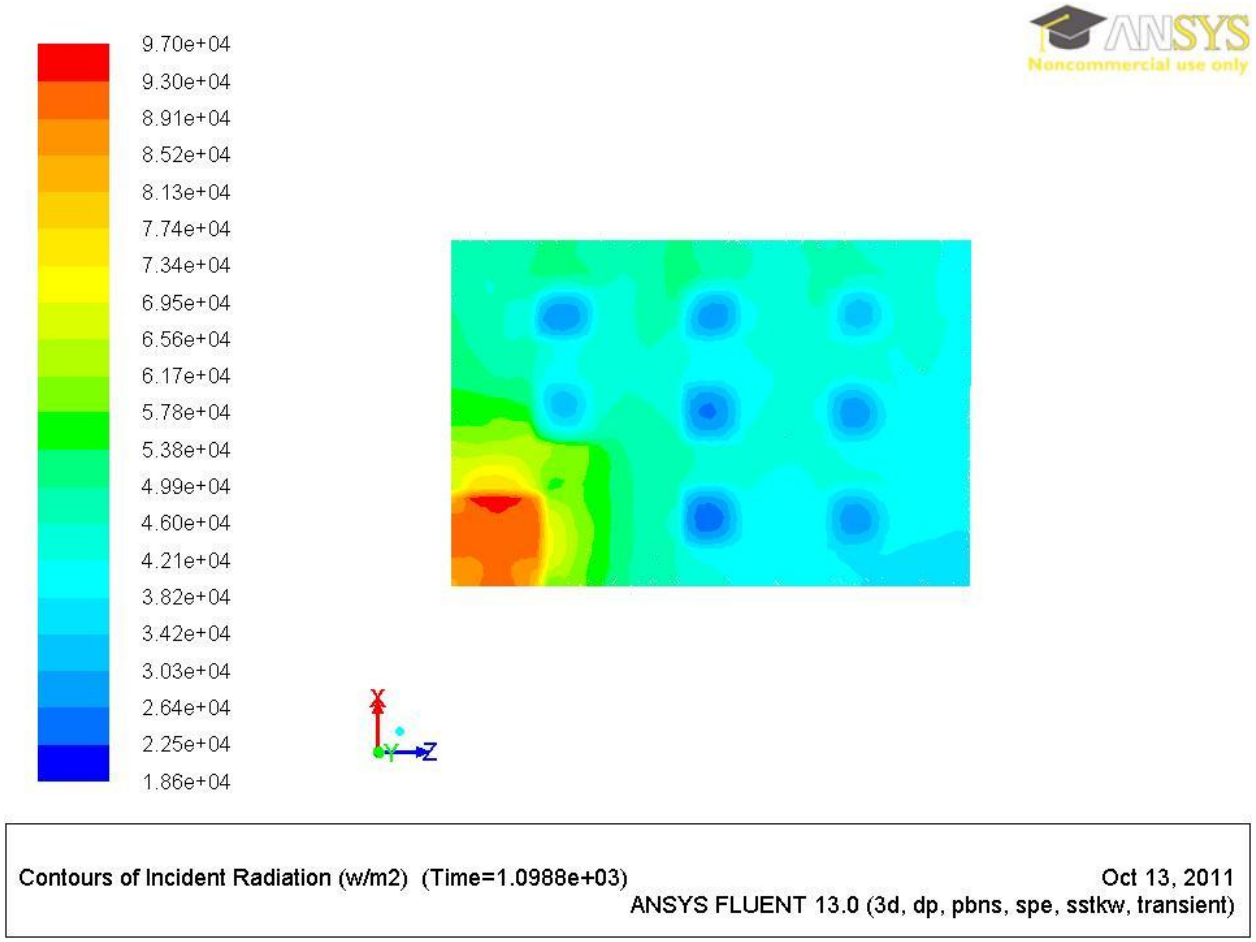

Figure 12 Radiation profile through the middle of the porous bodies.

4.1.3 Velocity profile

The velocity profile also confirms the results from Figure 11 regarding the strong inertia movement along the roof to the opposite corner of the furnace. This strong inertia movement across the roof can be seen in Figure 13.

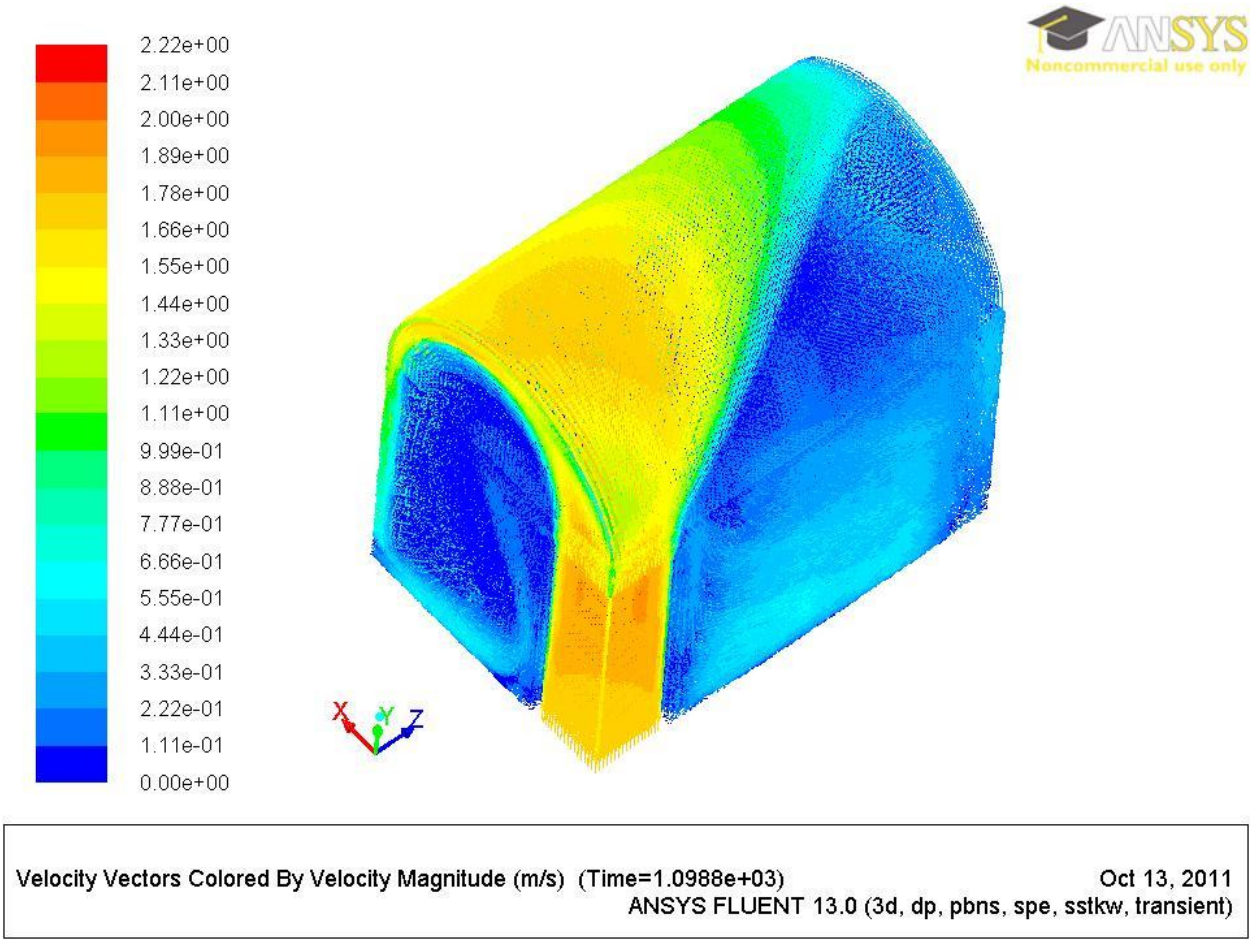

Figure 13 The flue gas velocity inside the furnace.

4.1.4 Simulation of evaporation

The Matlab simulations showed that the reaction for desorption and adsorption will be close to equilibrium after approximately 1100 seconds. The CFD simulations showed that the surface coverage of bounded water in the porous bodies decreased from 90% to 70% after 1100seconds. The initial water content in the porous bodies was 0,7852 kmol/m^3 and it decreased to 0, 4538 kmol/m^3, hence 42,2% of the initial water content evaporated during the first 1100seconds. The vapor pressure on the porous bodies will be approximately 150 Pa which is low according to the theory about vapor pressure on bounded water. Figure 14 show that the highest water content is found the center of some porous bodies.

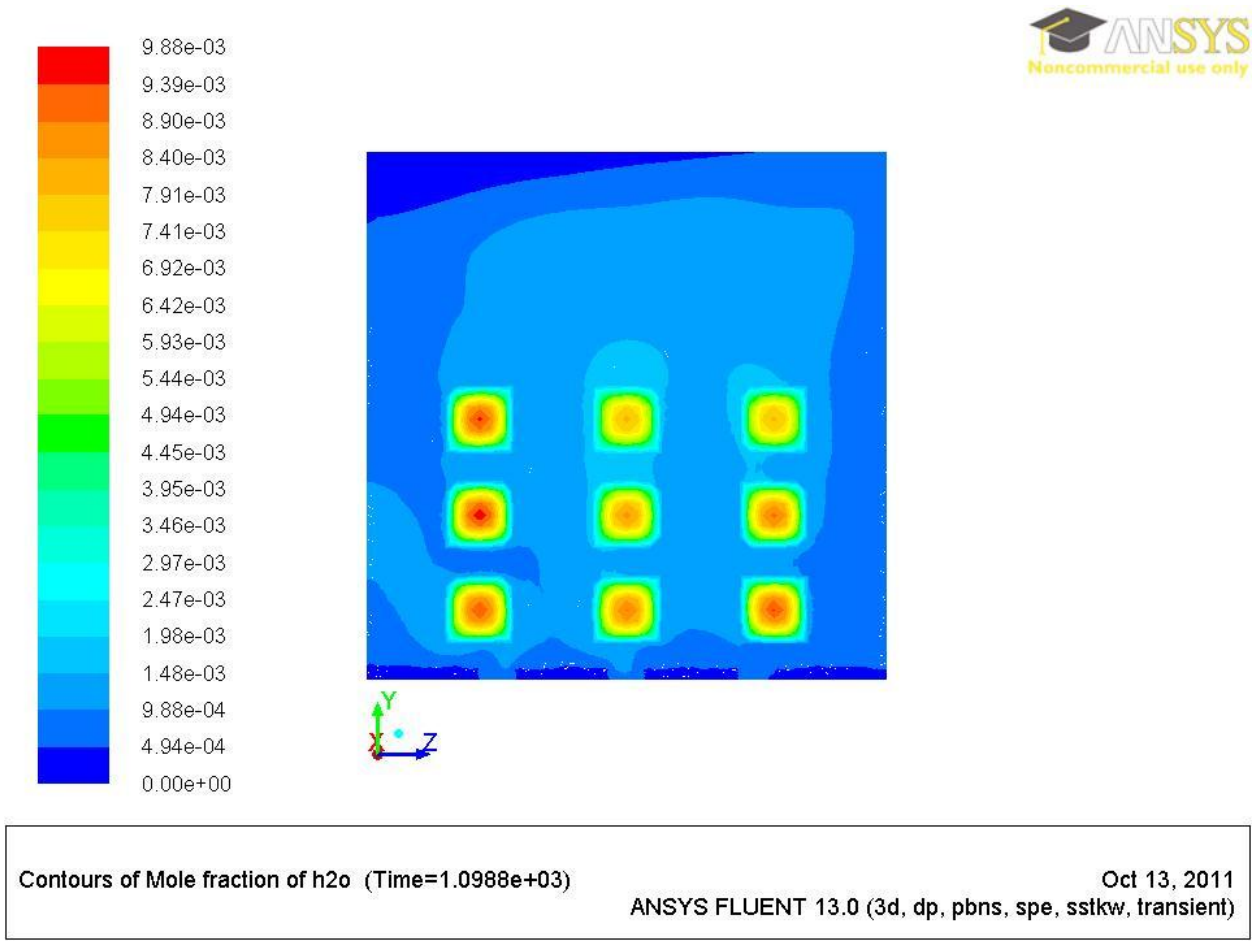

Figure 14 Mole fraction of H_2O after 1100 seconds simulation.

Results given from Fluent after 1100 seconds of simulation show that the rate of absorption is 126,47 mole/m^3s and the rate of desorption is 126,23 mole/m^3s. The rate of reaction is calculated per volume of porous body. This gives a net reaction rate of desorption of 0,24 mol/m^3s.

4.2 Results from study period in Indonesia

The results from the time spent in Indonesia are difficult to measure in hard fact. One result is increased knowledge about obstacles that can occur while planning a construction project. The transition from firewood to rice husk or coconut briquettes seems however to be running smoothly and the pottery makers seemed positive to try burning with the briquettes. Their attitude is of highest importance when it comes to obtaining the goal of an alternative fuel.

4.2.1 Construction of the furnace

Many issues need to be considered when a furnace will be constructed in Indonesia. It is difficult to find a good spot where the furnace could be built. It is also complex to decide how the money for this project should be spent as well as finding enough time to explore all the obstacles thoroughly. Collaboration between the academics planning the furnace and the pottery maker that will use it takes a lot of time to

establish. At the time of the end of this project, the furnace is scheduled to be built close to the end of 2011, which means a delay of approximately six month.

5 Conclusions

It was difficult to predict the outline of how the simulations should be performed. Many details had to be stripped down in order to create the model and it was complex to decide what factors had the largest impact on the overall process.

The results from the simulations indicate that it is possible to obtain quite an even temperature distribution inside the furnace with only one inlet. In reality, other factors such as uneven packing or large size distribution could be bigger contributors for an uneven temperature profile in the pottery and it is not sure a perfectly simulated temperature distribution will be as even in reality. A second inlet could be the answer to this issue but it is questionable if the unevenness is large enough for the extra work for the pottery maker that a second fireplace would bring.

The rate of reaction for adsorption and desorption was close to equilibrium after 1100 seconds which is exactly what was predicted with Matlab. This result is very satisfying and gives validation for the simulation of evaporation since two very different methods gave the same outcome.

Even though all simulations were performed with an inlet temperature of 1073K radiation proved to be significant. Prior to this project, it was thought that radiation only would be significant at higher temperatures meaning that this result is of great importance.

6 Discussion

Many more questions are of interest to find ways to improve the process of producing pottery. These questions can be divided into two categories, one regarding CFD and one regarding the practical work in Indonesia.

6.1 Further development of the CFD model

A baffle could be implemented in the geometry due to inertia movement that gives an uneven temperature distribution. A baffle would break the inertia movement and possibly give a more even temperature distribution, it would however give a larger pressure drop over the furnace.

In the obtained model, the pottery is approximated with rather large square elements and this approximation could be further refined to get results that possibly are closer to reality.

6.2 Further field studies in Indonesia

The construction of the obtained design is necessary to truly validate the results in this project. It would be of great interest to measure the temperature in different areas during a burning process. The temperature gauge should have a radiation protection to enable temperature measurements without radiation and compare to measurements without radiation protection were radiation is included.

It is of importance to continue with the efforts to open the pottery maker's minds and try other ways of burning pottery. This project is otherwise in vain since a constructed furnace will never be used if the pottery makers do not believe its improved properties.

7 Reference list

1. **Bengt Andersson, Ronnie Andersson, Love Håkansson, Mikael Mortensen, Rahman Sudiyo, Berend van Wachem.** *Computational Fluid Dynamics for Chemical Engineers.* Gothenburg : u.n. , 2008.

2. **James R. Welty, Charles E Wicks, Robert E. Wilson.** *Fundamentals of Momentum, Heat, and Mass Transfer.* United States of America : John Wilet & Sons, Inc., 2001.

3. **Callister, William D.** *Materials science and engineering, an introduction.* New York : John Wiley & Sons, Inc. , 2003.

4. **Jenkins, P. Mullinger and B.** *Industrial And Process Furnaces.* s.l. : Elsevier Ltd, 2008.

5. **Henley, J.D. Seader and E.J.** *Separation Process Principles.* United States of America : John Wiley & Sons, Inc., 2006.

6. **Norton, F. H.** *Refractories.* London : McGraw-Hill Book Company, Inc, 1949.

7. **Hellsten, S E Mörtstedt and G.** *Data och diagram.* Stockholm : Nordstedts Tryckeri, 1976.

8. **ANSYS, Inc.** ANSYS 13.0 Dokumentation. 2010.

8 Appendix

8.1 C++ code that defines the absorption coefficient

```
#include "udf.h"

DEFINE_GRAY_BAND_ABS_COEFF(abs_coeff,c,t,nb)

{

	real abs_coeff, NV_VEC(xc);


	C_CENTROID(xc,c,t);


	if ( THREAD_ID(t) == 20064)

		abs_coeff=1e5;


	else if ( THREAD_ID(t) == 10033)

		abs_coeff=1e5;

	else

		abs_coeff=0;

	return abs_coeff;

}
```

8.2 Matlab code for equilibrium calculations

```
clear all
close all
clc
global ka kd dH_vap q V_tank V_bodies n_h20 R T

V_tank=2*3*1.8+1^2*pi*3; %m3 volume of tank
V_bodies=0.4^3*24; %m3 volume of porous bodies
rho_bodies=2000; %kg/m3
wt_h20=0.2 ;%wt% of water in bodies, initially
m_bodies=V_bodies*rho_bodies %kg weight of porous bodies
MW_h2o=18; %kg/kmole mole weight of water
% n_h20=m_bodies*wt_h20/(MW_h2o*1e-3) %mole h20 per m3 porous body
n_h20=400/(MW_h2o)*1e-3 %kmole h20 per m3 porous body

R=8.31447e-3; %kJ/mole K gas constant
dH_vap=1.0*1404*1.5*MW_h2o*1e-3 %kJ/kg*kg/kmole=kJ/mole approximated heat of
vaporization for bounded water at 300 degree C (8)
%dH_vap=40 %kJ/kg*kg/kmole=kJ/mole approximated heat of vaporization for
bounded water at 300 degree C DoD

q=0.18; %m3/s
kd=50 ;
ka=60;
% tspan=[0 3600]
% tout=linspace(tspan(1),tspan(2))
[t y]=ode15s('hast',[0 1000],[0,0.9]);
% plot(t,y(:,2))
% hold on
figure(2)
plot(t,y(:,1))


function dydt=hast(t,y)

global ka kd dH_vap q V_tank V_bodies n_h20 R T

c=y(1);
theta=y(2);
T=200+273.15 +0.1*t %K
r_des=kd.*exp(-dH_vap./(R.*T))*theta
r_ads=ka*c*R*T*(1-0.9*theta)

dcdt= -q*c/V_tank+(r_des-r_ads).*V_bodies./V_tank;
dthetadt=-(r_des-r_ads)/n_h20;

dydt(1)=dcdt;
dydt(2)=dthetadt;
dydt=dydt';

% pause
```

8.3 Matlab code for air supply calculations

```
m_wood=500*(1-0.1124);          %kg dry wood/10 hour
H_wood=16770 ;                  %kJ/kg according to Cecilia's thesis
Q_furnace=m_wood*H_wood/(10*3600) %kJ/s Heat consumed in furnace
Q_ricehusk=4500*4.184;          %kJ/kg
A_inlet=0.25*0.25               %m2 inlet area in furnace
MW_wood=(6*12+10+16*5)*1e-3;    %kg/mole
MW_O2=32e-3;                    %kg/mole
MW_CO2=(12+32)*1e-3;            %kg/mole
MW_H2O=18e-3;                   %kg/mole
MW_N2=14e-3     ;               %kg/mole
cp_air=1.230                    %kJ/kg K at 1500 degree Celsius
MW_air= 28.96e-3   ;            %kg/mole
sigma=5.676e-8                  %W/m2K4 Stefan-Boltzmann constant

%Calculation of needed air supply
n_wood=m_wood/MW_wood;                  %moles of wood per batch
n_O2=6*n_wood;                          %moles of O2 required according to
C6H10O5 + 6O2 --> 6CO2 + 5H2O
m_O2=n_O2*MW_O2;                        %kg stoichiometric amount of O2
needed for one batch
m_air_tot=m_O2/0.231;                    %kg stoichiometric amount of air
needed for one batch from DoD p 20
m_air_tot_real=2*m_air_tot  ;           %kg amount of air with 100% excess
air.
m_air_real=m_air_tot_real/(10*3600) ;   %kg/s
rho_air=0.273;                          %kg/m3, temperature 1273 K
v_air=m_air_real/rho_air    ;           %m3/s
vel_air=v_air/A_inlet;                  %m/s inlet velocity

%Calculation of total inlet flow
m_CO2=6*n_wood*MW_CO2;                      %kg from combustion
m_H2O=5*n_wood*MW_H2O;                      %kg from combustion
m_N2=0.79*m_air_tot ;                       %kg inert
m_xs_air=2*m_air_tot ;                        %kg 100% xs air
m_vapor=500*0.1124;                         %kg the moist in the wood
evaporates
m_total=m_CO2+m_H2O+m_N2+m_xs_air+m_vapor;  %kg per batch
m_total_inlet=m_total/(10*3600)            %kg/s
in_vel=m_total_inlet/rho_air/A_inlet;       %m/s
%Calculation of inlet temperature
dT=Q_furnace/(m_total_inlet*cp_air)   ;     %K
Tin=dT+(273.15+30)          ;               %K assume 30 degree Celsius in
surroundings
Tin_real=800+273.15   ;                     %K actual input temperature set in
FLUENT
Q_real=(800-30)*(m_total_inlet*cp_air);     %kJ/s
%Calculation of needed coal brikets
m_briket_dry=(m_wood*H_wood)/Q_ricehusk ;   %kg
m_briket_total=m_briket_dry/0.9;            %kg assume 10% moist content

%Estimation of radiation vs convection
Q_radiation=sigma*(Tin_real^4-(400+273)^4)*1e-3                  %kW from WWW
Q_ratiation_inlet=Q_radiation/(1.8*.5*2)              %kW/m2
Q_convection=Q_real*.3/(1.8*.5*2)                           %kW/m2
```